

Formation of Two- and Three-Dimensional Hybrid Mesostructures from Branched Siloxane Molecules

Shigeru Sakamoto,[†] Atsushi Shimojima,[‡] Keiichi Miyasaka,^{§,||} Juanfang Ruan,[§] Osamu Terasaki,^{§,||} and Kazuyuki Kuroda^{*,†}

Department of Applied Chemistry, Waseda University, Ohkubo-3, Shinjuku-ku, Tokyo 169-8555, Japan, Department of Chemical System Engineering, The University of Tokyo, Hongo-3, Bunkyo-ku, Tokyo 113-8656, Japan, Structural Chemistry, Arrhenius Laboratory, Stockholm University, 10691 Stockholm, Sweden, and Graduate School of EEWS, Korea Advanced Institute of Science and Technology, Daejeon 305-701, Republic of Korea

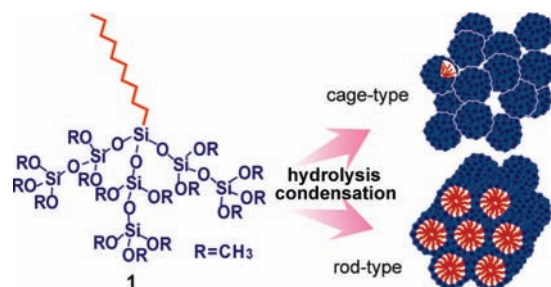
Received April 21, 2009; E-mail: kuroda@waseda.jp

The self-assembly route to hybrid inorganic–organic solids is of significant interest not only for fundamental research but also for the production of novel functional materials.^{1–3} Recently, ordered silica-based hybrid materials have been synthesized from organoalkoxysilanes by taking advantage of their intermolecular interactions and ability to form siloxane network by hydrolysis and polycondensation.^{4,5} The molecular design based on rich organo-silicon chemistry would permit fine-tuning of compositions, structures, and properties of the products. The design of amphiphilic siloxane-based molecules is promising for producing hybrid mesostructures with a long-range order. The structure can be controlled in part by varying the size of the siloxane head as well as the alkyl chain length.^{4,6} For example, trialkoxy- or trichloro-(alkyl)silanes form lamellar solids via hydrolysis and polycondensation,⁶ whereas tris(trialkoxysilyloxy)-(alkyl)silanes ($C_nH_{2n+1}Si(OSi(OR)_3)_3$, $n = 6–13$ (hereafter called “tetrasiloxane precursors”), can form mesophases consisting of rod-like assemblies such as 2D hexagonal phase.⁷ In view of the geometrical packing parameter,^{6a,8} further enlargement of the siloxane head should favor the formation of spherical assemblies, leading to structural diversity and complexity arising from packing variations; however, no such higher curvature mesophases have been observed for amphiphilic organosiloxanes without the aid of surfactants.

Here we report the design of a new precursor having three branching disiloxane units (**1** in Scheme 1) capable of forming 3D mesostructures with a cubic $Pm-3n$ and its orthorhombic and tetragonal variants $Cmmm$ and $P4_2/mnm$. A 2D hexagonal ($p6mm$) mesostructure was also formed by control of water content during self-assembly. The large, branched siloxane head of **1** is essential for the formation of such 3D mesophases, which have only been found in organic molecules and block copolymers with specific geometries,⁹ thus creating a novel research area of mesostructural design in silica-organic nanohybrid materials.

We have developed a facile route to the heptasiloxane precursor **1** by one-step silylation of decylsilanetriol⁷ with disiloxane species where $-OMe$ groups of hexamethoxydisiloxane ($(MeO)_3SiOSi(OMe)_3$) are partly replaced by more reactive $-Cl$ groups. Successful synthesis of **1** was confirmed by NMR and MS.¹⁰ Hydrolysis of **1** proceeded almost completely under acidic conditions in THF as confirmed by disappearance of the $SiOCH_3$ signals in the ^{13}C NMR spectrum. After diluting this hydrolyzed solution with more THF and water, the solution was cast and dried on a glass substrate

Scheme 1. Self-Assembly of the Precursor **1** into Two Types of Hybrid Mesostructures



to give a xerogel film (**1H_A**). Similarly, a hybrid solid, **1H_B**, was prepared by diluting with only THF under otherwise identical conditions.¹⁰

The powder XRD pattern of **1H_A** (Figure 1a) shows several peaks due to mesoscale periodicity. The TEM images (Figure 2) show that the material comprises different packing domains of cages with space groups of $P4_2/mnm$, $Pm-3n$, and their modulated mixture,¹⁰ among which the $P4_2/mnm$ is dominant. The packing of the cage domains is very coherent, which is evidenced by the FFT diffractograms (insets of Figure 2) that display well-resolved spots despite the presence of the mesostructural modulation and the relevant stacking faults.¹⁰ On the basis of the prevailing $P4_2/mnm$ symmetry, the lattice constants of the unit cell calculated from the FFT are $a = 12.8$ nm and $c = 5.3$ nm. These lattice constants are presumed to give the indexing of the present XRD peaks in Figure 1a. The packings with $P4_2/mnm$ and $Cmmm$ are explained from that with $Pm-3n$ by the occurrence of two-dimensionally periodic planar faults.¹¹ This same packing behavior and the relationship have since been described for liquid crystals^{9a} and a mesoporous silica (AMS-9) prepared with anionic surfactants and costructure directing agents.¹²

In contrast, the 2D hexagonal ($p6mm$) structure of **1H_B** was revealed by XRD and TEM showing either honeycomb or striped patterns depending on the electron incidents.¹⁰ The d_{10} spacing (2.69 nm) is smaller than that for the 2D hexagonal structure derived from the tetrasiloxane precursor with the same chain length ($d_{10} = 2.92$ nm),⁷ suggesting that **1H_B** has a smaller diameter of the rod-like assemblies. Although the larger siloxane head of **1** should lead to a thicker siloxane wall, the internal diameter should decrease because of the increased lateral distance and therefore lowered density of alkyl chains in the rods. These structural features were actually confirmed by nitrogen sorption data of the porous silica samples obtained by calcination.¹⁰

[†] Waseda University.

[‡] The University of Tokyo.

[§] Stockholm University.

^{||} Korea Advanced Institute of Science and Technology.

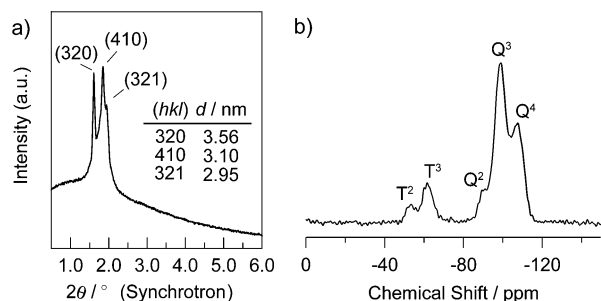


Figure 1. (a) Powder XRD pattern (collected in Spring-8, Japan) of **1H_A**, which is indexed based on the cell parameter determined from TEM observation. (b) ²⁹Si MAS NMR spectrum of **1H_A**.

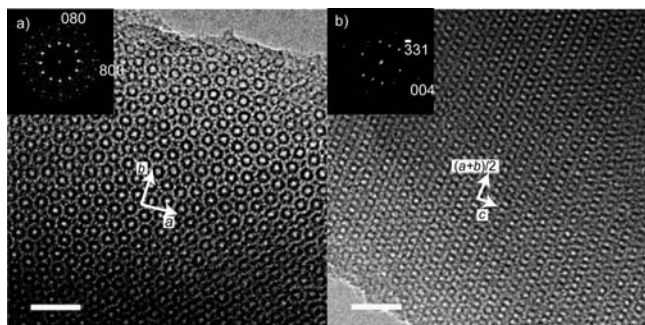


Figure 2. TEM images and FFT diffractograms of **1H_A** taken by a JEM-3010 microscope; (a) [001] and (b) [110] directions of *P4₂/mmm* space group. The italic symbols indicate the lattice vectors of the tetragonal lattice. Scale bar: 20 nm.

In both **1H_A** and **1H_B**, alkyl chains are in a similarly disordered state with mixed *trans*–*gauche* conformations, as suggested by the position of the $\nu_{\text{as}}\text{CH}_2$ bands (2930 cm^{-1}) in the IR spectra.¹⁰ Also, no difference was observed in the local structures of the siloxane networks. The solid-state ²⁹Si MAS NMR show similar spectra consisting of the T², T³, Q², Q³, and Q⁴ signals (T^x: $\text{CSi}(\text{OSi})_x(\text{OH})_{3-x}$; Q^y: $\text{Si}(\text{OSi})_y(\text{OH})_{4-y}$; see Figure 1b for **1H_A**).¹⁰ The presence of the T² signal indicates the partial cleavage of the Si–O–Si bonds in **1** during the synthesis. Nevertheless, the liquid-state ²⁹Si NMR spectrum of the hydrolyzed solution (data not shown) mainly showed the T³ signal, suggesting that uncleaved species were still predominant at this stage.

The variation of the mesostructures (**1H_A** and **1H_B**) with the water content in the precursor solution should be associated with the difference in the concentration of the hydrolyzed species after preferential evaporation of THF. Similar behavior has been found for silica–surfactant mesostructured films prepared by evaporation-induced self-assembly (EISA) processes.¹³

We also examined the use of a pentasiloxane precursor ($\text{C}_{10}\text{H}_{21}\text{SiMe}(\text{OSi}(\text{OMe})_2\text{OSi}(\text{OMe})_3)_2$), where one branching disiloxane unit of **1** is replaced with a methyl group. This precursor exclusively formed a 2D hexagonal phase as confirmed by XRD and TEM.¹⁰ The d_{10} spacing (3.04 nm) is larger by 0.35 nm than that of **1H_B**, which is explained by the smaller lateral distance of alkyl chains in the rods.

The present results suggest that alkylsiloxane mesophase is governed by both the size and configuration of the siloxane head. In contrast to the formation of well-ordered 3D mesophases from **1**, cubic-octasiloxane precursors ($\text{C}_n\text{H}_{2n+1}\text{Si}_8\text{O}_{12}(\text{OEt})_7$) yielded 2D hexagonal phases when $n = 16$ – 20 and the structure became disordered upon decreasing the chain length to $n = 10$.¹⁴ Although the number of Si atoms is similar among these two precursors, major differences exist in the rigidity and the number of hydrolyzable alkoxy groups. The maximum number of –OH groups generated by hydrolysis is much larger for **1** (15 –OH per molecule) than for the octasiloxane precursors (7 –OH per molecule). Thus, the hydrolyzed **1** should be more amphiphilic and, hence, capable of forming well-ordered mesostructures.

In conclusion, we have demonstrated the formation of 3D tetragonal (and cubic) as well as 2D hexagonal mesostructures from a branched heptasiloxane precursor, providing deeper insight into the relationship between molecular structure and self-assembled mesostructures of alkylsiloxane amphiphiles. The modification of the organic counterpart is under study to achieve more sophisticated structures with specific functions.

Acknowledgment. This work was supported in part by the Global COE program, a Grant-in-Aid for Scientific Research on Priority Areas from MEXT, Japan, and the WCU program of the Korean Government (MEST). O.T. acknowledges the Knut and Alice Wallenberg Foundation for the support to EM centre of Stockholm University. We are grateful to Mr. S. Nasu, Ms. M. Sakurai, Mr. K. Kawahara (Waseda Univ.), and Ms. J. Du (Queen's Univ., Canada) for experimental help and suggestions.

Supporting Information Available: Experimental section, additional XRD, NMR, IR, and TEM data. This material is available free of charge via the Internet at <http://pubs.acs.org>.

References

- (1) Colfen, H.; Mann, S. *Angew. Chem., Int. Ed.* **2003**, *42*, 2350.
- (2) Descalzo, A. B.; Martinez-Manez, R.; Sancenn, F.; Hoffmann, K.; Rurack, K. *Angew. Chem., Int. Ed.* **2006**, *45*, 5924.
- (3) Hoffmann, F.; Cornelius, M.; Morell, J.; Fröba, M. *Angew. Chem., Int. Ed.* **2006**, *45*, 3216, and references therein.
- (4) Shimojima, A.; Kuroda, K. *Chem. Rec.* **2006**, *6*, 53.
- (5) For example, (a) Moreau, J. J. E.; Vellutini, L.; Wong Chi Man, M.; Bied, C. *J. Am. Chem. Soc.* **2001**, *123*, 1509. (b) Boury, B.; Corriu, R. J. P. *Chem. Commun.* **2002**, 795.
- (6) (a) Huo, Q.; Margolese, D. I.; Stucky, G. D. *Chem. Mater.* **1996**, *8*, 1147. (b) Parikh, A. N.; Schivley, M. A.; Koo, E.; Seshadri, K.; Aurentz, D.; Mueller, K.; Allara, D. L. *J. Am. Chem. Soc.* **1997**, *119*, 3135. (c) Shimojima, A.; Sugahara, Y.; Kuroda, K. *Bull. Chem. Soc. Jpn.* **1997**, *70*, 2847.
- (7) Shimojima, A.; Liu, Z.; Ohsuna, T.; Terasaki, O.; Kuroda, K. *J. Am. Chem. Soc.* **2005**, *127*, 14108.
- (8) Wan, Y.; Zhao, D. *Chem. Rev.* **2007**, *107*, 2821.
- (9) (a) Ungar, G.; Zeng, X. B. *Soft Matter* **2005**, *1*, 95. (b) Hayashida, K.; Dotera, T.; Takano, A.; Matsushita, Y. *Phys. Rev. Lett.* **2007**, *98*, 195502. (c) Thomas, E. L.; Anderson, D. M.; Henkee, C. S.; Hoffman, D. *Nature* **1988**, *334*, 598.
- (10) See Supporting Information for details.
- (11) Hiraga, K.; Hirabayashi, M.; Terasaki, O.; Watanabe, D. *Acta Crystallogr.* **1982**, *A38*, 269.
- (12) Garcia-Bennett, A. E.; Kupferschmidt, N.; Sakamoto, Y.; Che, S.; Terasaki, O. *Angew. Chem., Int. Ed.* **2005**, *44*, 5317.
- (13) Cagnol, F.; Grosso, D.; Soler-Illia, G. J. de A. A.; Crepaldi, E. L.; Babonneau, F.; Amenitsch, H.; Sanchez, C. *J. Mater. Chem.* **2003**, *13*, 61.
- (14) Shimojima, A.; Goto, R.; Atsumi, N.; Kuroda, K. *Chem.–Eur. J.* **2008**, *14*, 8500.

JA903176K